

# Flow transients in the post-noon ionosphere: The role of solar wind dynamic pressure

A. Thorolfsson, J.-C. Cerisier<sup>1</sup>

Centre d'étude des Environnements Terrestre et Planétaires, Saint-Maur, France

M. Pinnock

British Antarctic Survey, Natural Environment Research Council, Cambridge, United Kingdom

**Abstract.** SuperDARN HF radar, magnetometer and satellite data are used to study ionospheric convection flow bursts in the sunward return flow in the 12-15 MLT auroral region. A comparison between the latitudinal position of the flow bursts and the position of the open/closed field line boundary shows that the sunward bursts occur on closed field lines. The bursts occur simultaneously with poleward motions of the convection reversal boundary. Decreases in the solar wind dynamic pressure are shown to correlate well with the flow bursts. Comparison of radar and magnetometer data shows that these observations can be explained in terms of the global current model proposed for sudden expansions of the magnetosphere [Araki and Nagano, 1988]. The sunward flow bursts are shown to be consistent with the high-latitude dusk to dawn electric field predicted by the model during pressure decreases.

## Introduction

The study of transient phenomena in the ionosphere is an important key to the understanding of solar wind interactions with the magnetosphere. The most important driving mechanism of ionospheric flow is without doubt magnetic reconnection at the magnetopause. Candidate signatures of pulsed and localized reconnection at the dayside magnetopause (called Flux Transfer Events, or FTEs) have been studied extensively. These studies include satellite data [e.g. Russell and Elphic, 1978, 1979; Rijnbeek *et al.*, 1984], data from ground instruments such as incoherent, VHF and HF-radars [e.g. Lockwood *et al.*, 1990; Goertz *et al.*, 1985; Pinnock *et al.*, 1993, 1995], and a combination of optical and ground magnetic data [e.g. Moen *et al.*, 1995; Øieroset *et al.*, 1996, 1997]. The occurrence of FTEs is known to depend on the  $B_z$  component of the interplanetary magnetic field (IMF), requiring that  $B_z$  be southward (negative) or only slightly northward (shear angle above  $75^\circ$ ) [Berchem and Russell, 1984]. FTEs have a mean recurrence period of about 8 minutes when  $B_z$  is firmly southward [Lockwood *et al.*, 1989]. The  $B_y$  component influences the evolution of the recently reconnected flux tubes. The magnetic tension pulls the tube towards the

afternoon (morning) sector in the northern hemisphere for a negative (positive)  $B_y$  [Cowley *et al.*, 1991; Sandholt *et al.*, 1993; Karlson *et al.*, 1996].

HF-radar velocity signatures attributed to FTEs [Pinnock *et al.*, 1993, 1995] appear as elongated channels of accelerated flow, with peak flow velocities up to 3 km/s. As predicted by models [Southwood, 1987], the flow velocity inside the flow channel is of the same order as the velocity of the channel itself [Pinnock *et al.*, 1993]. Identification of FTEs from ground magnetometer signatures alone is difficult. Øieroset *et al.* [1996, 1997] have shown examples of magnetometer signatures associated with poleward moving auroral forms (Sandholt *et al.* [1986]), believed to be the optical signatures of FTEs. These authors observe poleward progressing deflections of the H-component at high auroral latitudes. At low- and sub-auroral latitudes, the magnetic signatures are typical of field line resonances. Whether or not the resonances are directly driven by reconnection remains an open debate.

Another source of transient phenomena are solar wind dynamic pressure changes. They have been shown to produce transient magnetosphere and ground signatures that closely resemble signatures of FTEs [Sibeck, 1990; Sibeck and Croley, 1991; Kivelson and Southwood, 1991]. Several authors [e.g. Glassmeier *et al.*,

<sup>1</sup> Also at Université Pierre et Marie Curie, Paris, France

1989; *Glassmeier and Heppner*, 1992; *Lühr et al.*, 1996] have also shown ground magnetometer observations with FTE-like signatures, the so-called Traveling Convection Vortices (TCVs). These vortices have a rather large scale size (about 1000 km) and travel tailwards at speeds of 3-7 km/s. One characteristic observation is that in the center of the double-vortex structure, plasma flow is nearly perpendicular to the direction of motion, as opposed to FTE model signatures [*Southwood*, 1987] where both velocities are parallel. *Glassmeier and Heppner* [1992] and *Kivelson and Southwood* [1991] predicted that this type of signature is consistent with pressure changes being the driving mechanism.

The balance between the solar wind plasma pressure and the magnetic pressure exerted by the magnetosphere is achieved by a dawn to dusk current flowing across the dayside magnetopause. A sharp decrease (increase) in pressure gives rise to an expansion (compression) of the magnetosphere, which is accompanied by a dusk to dawn (dawn to dusk) counter-current [see for example *Araki*, 1994, and references therein]. This perturbation launches a fast mode expansional (compressional) wave that propagates radially towards the ionosphere. Because of the inhomogeneity of the magnetosphere, the fast mode couples to an Alfvén mode that propagates along the magnetic field lines.

Due to a faster propagation speed of the Alfvén wave, compared to the radial expansional (compressional) wave, the first response of the ionosphere (called the preliminary impulse, or PI) is due to the field aligned currents (FACs) associated with the Alfvén wave [*Wilken et al.*, 1982]. For a pressure decrease, the FACs flow out of the ionosphere on the dusk side in the northern hemisphere and into the ionosphere on the dawn side. This creates a twin vortex current system in the ionosphere, with a clockwise Hall current vortex on the morning side and an anti-clockwise vortex on the afternoon side (in the sun-earth inertial frame). The FACs flow in the opposite sense for pressure increases, and the sense of rotation for the current vortices is reversed.

As the expansional (compressional) wave propagates towards the earth, the magnetic field in the magnetosphere will be decreased (increased). This effect has been measured with geosynchronous satellites [e.g. *Erlundson et al.*, 1991; *Korotova et al.*, 1999]. Once the fast wave hits the ionosphere, the H-component of the ground magnetic field starts to decrease (increase), in the case of a pressure decrease (increase).

After the expansional (compressional) front has passed the earth, the magnetospheric convection readjusts to the new compressed state. The FACs associated with this adjustment (called the main impulse, or MI) flow into the ionosphere on the dusk side in the northern hemisphere and out of the ionosphere on the dawn side for a pressure decrease. This creates an ionospheric cur-

rent vortex system that has an inverse sense of rotation compared with the preliminary impulse.

The ground magnetometer response to these combined changes are mainly detected in the H-component. *Araki and Nagano* [1988] showed that in the afternoon sector at mid- and auroral latitudes, the preliminary response to a sudden pressure decrease (also called SI<sup>-</sup>) is typically a short positive pulse followed by a broad negative one. In the morning sector, the signatures are inverse: a short negative pulse followed by a broad positive pulse. For a sudden pressure increase (called SC or SI), the afternoon magnetometers show a short negative pulse, followed by a positive one. Furthermore, at latitudes higher than the FACs, the sign of the magnetic pulses is reversed compared with the mid- and auroral regions [e.g. *Araki*, 1994]. This type of ionospheric response to sudden pressure increases or decreases will be referred to as the SI/SI<sup>-</sup> model.

*Glassmeier and Heppner* [1992] show an example where low-latitude magnetometers from dawn to dusk respond simultaneously to a pressure increase. Immediately after that, mid- and high-latitude magnetometers from dawn to noon showed a tailward propagating TCV. *Kivelson and Southwood* [1991] propose that a localized single-step change in pressure produces a pair of vortices on the same side of the magnetosphere, in agreement with the TCV picture. This localized picture is different from the global *Araki* [1994] picture, which supposes also two vortices, but one on each side of the magnetosphere.

*Araki* [1994] evokes also examples of nearly simultaneous magnetometer responses to sudden commencements at very different local times and also at a wide range of latitudes near noon. A particular example shows a response at a high-latitude station near 15:00 MLT and a response less than one minute later at a low-latitude station near 01:00 MLT [*Kikuchi*, 1986]. This fast propagation is thought to be due to a waveguide mode between the ionosphere and the earth [*Kikuchi et al.*, 1978; *Kikuchi*, 1986].

In this paper, the response of the ionospheric convection to solar wind pressure decreases is studied. The experimental data are from a period when a high time resolution mode was used for the Stokkseyri SuperDARN HF radar. The data are used to study dayside ionospheric velocity flow bursts in the return flow from the nightside. The existence of the bursts will be discussed in terms of dynamic processes at the magnetopause, namely reconnection and pressure changes.

The paper is organized in the following manner. First, the instruments used in the study are introduced. Then a representative case study (January 8, 1998) is presented in detail. Finally, the results are analyzed and possible source mechanisms are discussed.

## Instruments

The Stokkseyri Iceland radar is a part of the extended network of HF backscatter radars called SuperDARN (Super Dual Auroral Radar Network) [Greenwald *et al.*, 1995]. In normal mode, the Stokkseyri radar steps through 16 adjacent azimuthal directions (beams), separated by  $3.3^\circ$ . This beam separation is approximately equal to the beam width. The field of view (FOV) of the radar is above Greenland and north-eastern Canada (cf. figure 1). The SuperDARN radars measure line-of-sight flow velocities, and operate in pairs. This setup permits velocity measurements to be combined and yield flow vectors. On January 8, 1998, the radar was operated in a special mode, providing a high time-resolution on three of the sixteen beam directions (beams 7, 9 and 11, cf. figure 1). The SuperDARN data are presented in the AACGM coordinates, which are altitude-adjusted CGM coordinates (see *Baker and Wing* [1989]). To make comparison with radar data easier, high-latitude ground magnetic coordinates will also be expressed with this system.

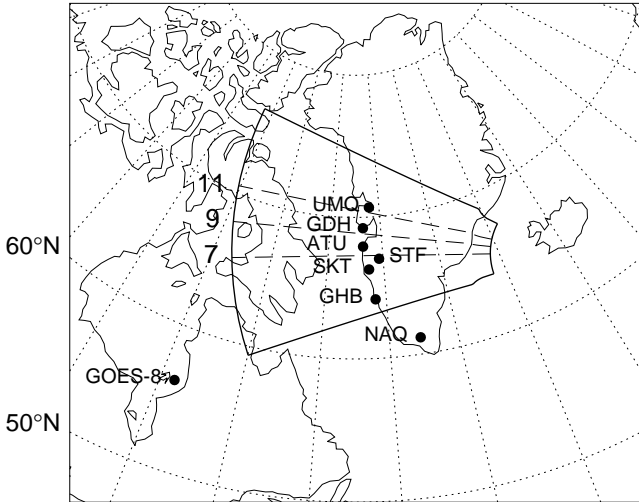


**Figure 1.** The field of view of the Stokkseyri radar (thick lines), plotted in geographical coordinates. The direction of beams 7, 9 and 11 are plotted with dashed lines. Several stations from the Greenland magnetometer chain are shown with points. The magnetic field line footprint of the GOES-8 satellite position is also shown with a point.

Data from several magnetometers are used in the study. The low- and mid-latitude magnetometers are Brorfelde in Denmark, Mbour in Senegal, Addis Ababa in Ethiopia, Alibag in India, Kakioka in Japan and Honolulu in Hawaii. High-latitude magnetometer data are from the Greenland magnetometer chain, a part of which is situated in the FOV of the Stokkseyri radar.

Solar wind data on January 8, 1998, are obtained from the Wind satellite, which is about  $228 R_E$  upstream from the Earth. GOES-8 is a geosynchronous satellite positioned at local time UT-5 ( $285.5^\circ$  geographical longitude). Total magnetic field data from the satellite are presented. NOAA-14 is a low-altitude (870 km) polar orbiting satellite that provides electron and ion fluxes in the 0.3 to 20 keV range. Data from a conjunction with the Stokkseyri radar FOV are used to determine the projections of magnetospheric boundaries in the ionosphere.

## Observations

### Solar wind conditions

The first four panels in figure 2 show the IMF components  $B_x$ ,  $B_y$ ,  $B_z$  (in GSM coordinates) and the solar wind dynamic pressure measured by Wind on January 8, 1998, plotted on a time axis lagged by 52 minutes (see below). The main IMF features are that  $B_y$  is negative throughout the 13:00 to 16:00 UT period and  $B_z$  is negative or around zero. The pressure varies between 3 and 8 nPa and shows several 30% - 40% changes on a time scale of 10 minutes or less. Panel 5 in the figure shows the total magnetic field measured by GOES-8. As can be seen, this parameter correlates rather well with the pressure detected at Wind, especially when we bear in mind that Wind was approximately  $228 R_E$  upstream in the solar wind. The GOES-8 magnetic field and Wind pressure data were cross-correlated to determine the mean timelag from Wind to the magnetopause. The lag was calculated using a sliding one-hour window, and a lag of  $52 \pm 5$  minutes was obtained. This lag has been added to all the Wind parameters in figure 2.

For comparison, the timelag can be calculated from solar wind parameters and the position of the Wind satellite. Using a solar wind front angle of  $45^\circ$  (parallel to the IMF direction), an approximately 60 minute delay is obtained. This is of the same order as the lag obtained with direct correlation and the difference is explained by fluctuations of propagation velocities and front angles.

There is a significant departure from the correlation at 15:36 UT, where GOES-8 detects a rather sharp decrease in  $B$  (probably indicating a pressure decrease) when Wind detects no change in pressure. A comparison with low-latitude magnetometer data will help to determine the cause of this change (see next section).

### Ground magnetometer data

**Mid- and low-latitude signatures** To confirm that the magnetic signatures measured with GOES-8 are due to pressure changes, data from several mid- and low-latitude magnetometers were examined. Figure 3 shows the GOES-8 total magnetic field and the

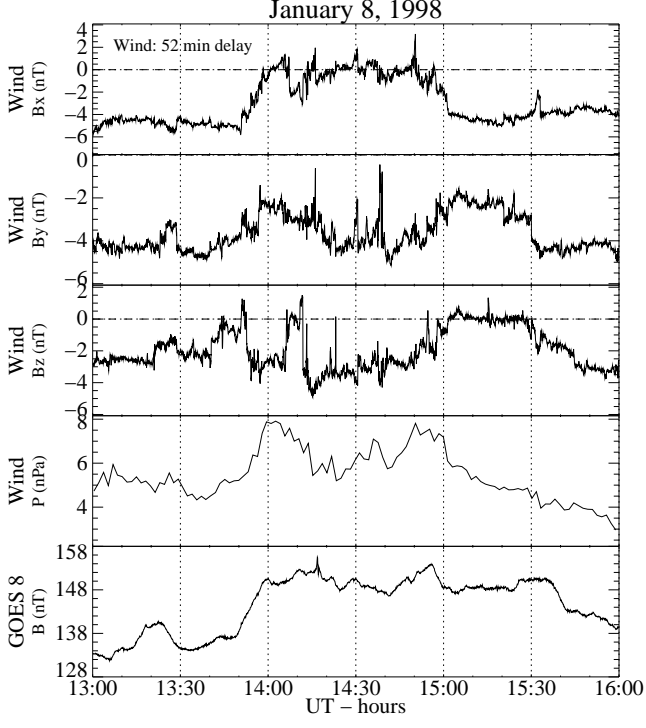


**Figure 2.** IMF  $B_x$ ,  $B_y$ ,  $B_z$  and solar wind pressure from Wind compared with the total magnetic field at GOES 8.

H-component of six magnetometer stations. The positions of these stations are shown in table 1. The first station (BFE) is in the figure is at mid-latitudes, and the other stations are at low-latitudes, ordered from the early afternoon sector (MBO) through midnight (KAK) to the early morning sector (HON). The dashed vertical lines in the figure indicate the onset of three supposed pressure changes inferred from GOES-8 data (13:49:30, 14:56 and 15:36 UT). The figure shows that an excellent correlation between GOES-8 data and the H-components for stations at very different MLT locations.

The global scope of these magnetic variations indicates that they are caused by compression and expansion of the whole magnetosphere, which points strongly towards pressure control. As an example, the sharp rise at all magnetometers after 13:49:30 UT is simultaneous, which shows that the effect is truly global, and that it propagates quickly to all ground stations. Since all large changes are detected both with GOES-8 and the ground magnetometers, the idea that pressure is the controlling factor in GOES-8 signatures is verified. The GOES-8 signatures can thus safely be used as a proxy for the dynamic pressure at the magnetopause. One also notes that the short negative deflection at 13:51 UT at BFE, which precedes the rise of the H-component, can be interpreted as the preliminary response of a pressure

increase, consistent with the SI/SI<sup>-</sup> model.

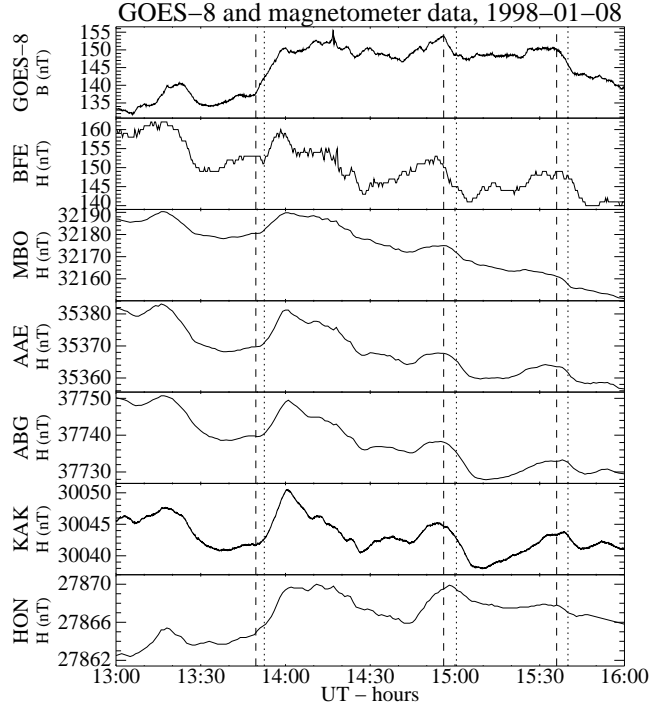


**Figure 3.** The total magnetic field at GOES-8 and the H-component of several mid- and low-latitude magnetic stations on January 8, 1998. BFE, MBO, AAE and ABG are in the afternoon sector, KAK just before local midnight and HON in the early morning sector. A baseline of 17130 nT has been subtracted from BFE data.

**Greenland chain** Figure 4 shows the component in the direction of magnetic north (later referred to as the  $X_M$  component) of the magnetometers on the west coast of Greenland between 13:40 and 16:00 UT. This particular projection of the horizontal magnetic component is chosen to facilitate the comparison with radar data. The stations are ordered in decreasing magnetic latitude, from top to bottom. The dashed vertical lines show the onset of the three pressure changes measured by GOES-8 referred to earlier.

Following the 13:49:30 UT pressure increase at GOES-8, the Greenland magnetometer chain shows a typical SI response. The preliminary response (PI) is detected from about 13:50 UT (positive deflection at higher latitudes), and the main response (MI) from about 13:52:30 UT (negative deflection at higher latitudes). The start of these responses is shown with dotted lines in figure 4. The preliminary impulse lag from GOES-8 to these high-latitude magnetometers is thus approximately 30 seconds, which agrees with previous results [Wilken et al., 1982]. The preliminary and main magnetic deflections are reversed between the low-

**Table 1.** Position of the magnetic stations referred to in figure 3. The approximate MLT of the stations is shown as a function of UT in the format hh:mm. The time resolution of the data is given in the last column.

Station name	Acronym	GLAT	GLON	MLAT	MLT	Res.
Brorfelde	BFE	55.6	11.7	52.0	UT-01:45	20 s
Mbour	MBO	14.4	343.0	1.6	UT+00:34	60 s
Addis Ababa	AAE	9.0	38.8	-1.2	UT-01:33	60 s
Alibag	ABG	18.6	72.9	11.8	UT-05:05	60 s
Kakioka	KAK	36.2	140.2	29.1	UT-08:55	1 s
Honolulu	HON	21.3	202.0	21.6	UT+11:09	60 s

est latitude magnetometer (NAQ,  $66^{\circ}$  MLAT) and those at higher latitude (UMQ and GDH, around  $76^{\circ}$  MLAT). This behavior agrees with the proposed SI/SI<sup>-</sup> current model [e.g. *Araki*, 1994]. The transition between these opposite responses takes place at around  $70^{\circ}$  MLAT. The signs of both the preliminary and main impulse correspond also to the predictions of the SI/SI<sup>-</sup> model in the noon and afternoon regions [*Araki*, 1994].

The response to the decrease in pressure detected with GOES-8 at 15:36 UT can be seen in the data as a change in the  $X_M$ -component between about 15:36 and 15:50 UT. The dotted vertical lines at 15:36:30 and 15:40 UT denote approximately the beginning of the preliminary and main impulse, respectively. The signature at all magnetometers is close to being opposite to that following the 13:49:30 UT event, in agreement with the reversed sign of the pressure variation. At GDH and UMQ, the preliminary response can be seen as a negative deflection, followed by the positive deflection due to the main response. At ATU, STF and SKT, the shape of the main response changes gradually with decreasing latitude. The duration of the positive deflection becomes shorter, and the maximum response is reached earlier at lower latitudes. This behavior is also evident for the 13:49:30 UT event, and was also observed by *Araki* [1994] (cf. his figure 7). At the lowest latitude station (NAQ), the reversed signature (compared with the high latitude stations) of both the preliminary and the main responses is not as clearly detected as for the 13:49:30 UT event. Because of this, the latitude of the SI/SI<sup>-</sup> current reversal boundary is difficult to estimate, but it is probably lower than  $70^{\circ}$  MLAT.

As already mentioned, the response transition between lower and higher latitude magnetometers stations leads to different rise and peak times of the  $X_M$ -component. This magnetic component is mainly affected by the east-west Hall current in the ionosphere. An increased eastward Hall current corresponds to an increase in the  $X_M$  component, and an increased westward plasma flow, if uniform height-integrated conductivities are assumed. The different rise and peak

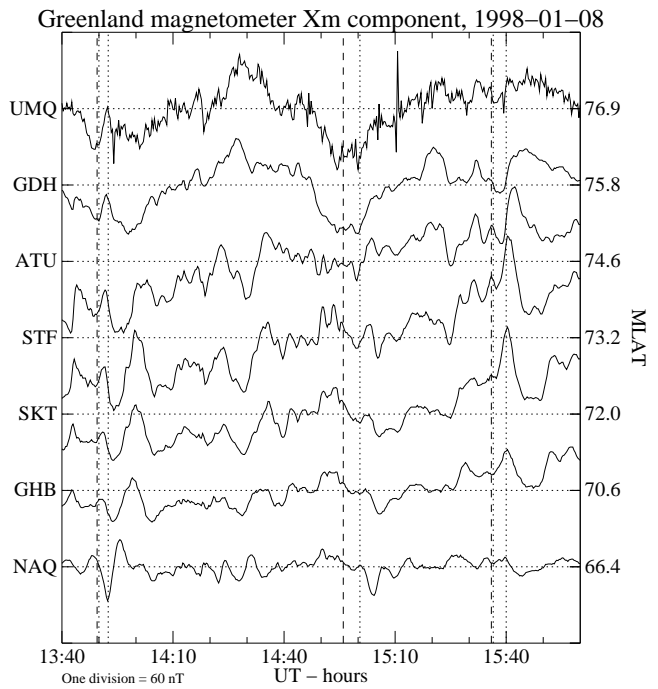


**Figure 4.** The  $X_M$  component of several Greenland magnetometers between 14:40 and 16:00 UT on January 8, 1998. The magnetic latitude of each station is given to right of the data. The height of one row denotes 60 nT. The dashed vertical lines indicate the onset of significant pressure variations measured by GOES-8. The dotted vertical line at 15:00:30 UT indicates a possible start of a main impulse. The dotted vertical lines after 15:36 UT denote the start of the preliminary and main impulse in response to the 15:36 UT pressure decrease.

times of the signatures in figure 4 indicate that the plasma flow does not react simultaneously at all latitudes. The difference is clearest between the stations STF and ATU. The lag from STF to ATU is approximately 97 s and 78 s for the rise and peak times, respectively. We will show below that this lag is also

detected in the plasma flow by the Stokkseyri radar. The magnetometer data predict peaks in the westward plasma velocity at about 15:40:30, 15:41 and 15:42 UT at 70.6°, 73.2° and 74.6° MLAT, respectively. This further indicates that there could be a 4 to 6 minute lag from the beginning of the decrease of pressure, measured by GOES-8, to the maximum response in radar signatures at these latitudes. Incidentally, this lag corresponds also to the typical fall time of the magnetic field detected with GOES-8 at 14:56 and 15:36 UT.

The magnetometer signatures following the 14:56 UT pressure decrease at GOES-8 are not as clear as those discussed above. A part of the reason might be that the IMF  $B_z$  component changed (from negative to around zero) at the same time as the pressure decreased. A gradual effect of the  $B_z$  change is observed in the magnetometer data at higher latitudes. A slower rate of reconnection leads to weaker flow in the polar cap, and thus a smaller westward ionospheric current poleward of the CRB in the afternoon. The signatures at UMQ and GDH show a positive drift of the  $X_M$  component, in agreement with this picture. Because of this drift, it is not clear whether the sharp rise at about 15:00 UT is due to the main response of a pressure effect (c.f. the signatures at 15:40 UT) or the change in  $B_z$ . There is no discernible preliminary response to the pressure decrease at any of the magnetic stations, but features of a main response are present at lower latitudes. The signatures at NAQ show a sharp dip the in  $X_M$  component and the stations from GHB to ATU show positive deflection that increases in amplitude and lag with increasing latitude. These signatures are similar to the main response at 15:40 UT, and indicate a pressure effect. Peak values of the westward plasma velocity are predicted at about 15:03 and 15:03:30 UT at 73.2° and 74.6° MLAT, respectively.

## Radar signatures

In the 14:00 to 16:00 UT period, the IMF has a negative  $B_y$  and a mainly negative  $B_z$  component. The expected large-scale plasma flow in the ionosphere is therefore a two-cell pattern, with a crescent-shaped cell on the afternoon side.

As can be seen in figure 5a, the beams of the Stokkseyri radars are directed to the west and northwest. Since the radar measures only line-of-sight (l-o-s) velocities of the plasma flow in the ionosphere, the measurements are generally more sensitive to zonal flow than meridional. The figure shows that at close ranges, the radar detects negative velocities (flow away from the radar). At further ranges, the velocity becomes positive (flow towards the radar). This is in good agreement with a crescent-shaped flow cell, the negative velocities representing the return plasma flow from the magnetotail (sunward flow), and positive velocities representing the flow driven into the polar cap (probably by recon-

nection). The convection reversal boundary (CRB) can be clearly seen where l-o-s velocities change from negative to positive. At the time of the scan in figure 5a, the CRB is observed at around 76° MLAT, between 12:00 and 13:30 MLT.

Plate 1 shows the total magnetic field data from GOES-8 (panel 1) and radar data from Stokkseyri (panels 2 to 4) between 14:00 and 16:00 UT. The satellite moves from 9:00 to 11:00 MLT during that period. The main portion of the radar data comes from the UT-0.5 to UT-2.5 region, which is in the noon and early afternoon sector for the period under study. The data in the three beams show that the westward flow (negative velocities) is very dynamic. Two large flow bursts (red-coded velocities) can be detected between 15:00 and 16:00 UT, and many smaller bursts are seen in the whole period. During the burst starting at about 15:04 UT, the l-o-s velocities attained about -1.5 km/s and -1.7 km/s in beams 9 and 7, respectively. This is more than twice as high as the velocity between burst, which is approximately -0.7 km/s. Since the l-o-s velocity is a projection of the plasma flow velocity onto the beam directions, these figures are a lower limit for the actual velocity. Assuming that beams 7 and 9 are detecting the same plasma flow regime, then the greater velocity in beam 7 implies that the flow is close to zonal, as expected for the return flow in the afternoon crescent-shaped cell. A similar result is found for the burst starting at about 15:40 UT.

Another striking feature of the data are the changes in latitude of the CRB, mainly detected in beams 9 and 11. These motions are clearly seen in the 14:00 to 15:00 UT period, and changes of up to 1.4° in 5 minutes are detected. The signatures in beam 9 lead those in beam 11 by about 90 seconds. The distance between these beams at 76° MLAT is about 180 km, which indicates a tailward propagation of 2 km/s of these features. It is also clear that velocity enhancements are associated with these variations of the CRB. Poleward displacements of the CRB are always accompanied by stronger sunward (negative) velocities equatorward of the CRB. The tailward (positive) velocities also grow stronger poleward of the CRB when its latitude decreases, although the effect is less pronounced. These velocity changes are most easily observed above and below the CRB between 14:45 and 15:10 UT.

A comparison of the GOES-8 and radar data (beams 11 and 9) shows that the major changes in the total magnetic field (and thus the solar wind pressure) correlate well with changes in the l-o-s velocities. The two largest pressure decreases (vertical dashed lines in plate 1) are both followed by large sunward flow bursts, lagging the pressure change by several minutes. The highest rise in pressure, between 14:42 and 14:56 UT, corresponds also to the lowest position of the CRB and the highest tailward velocities. Smaller changes in

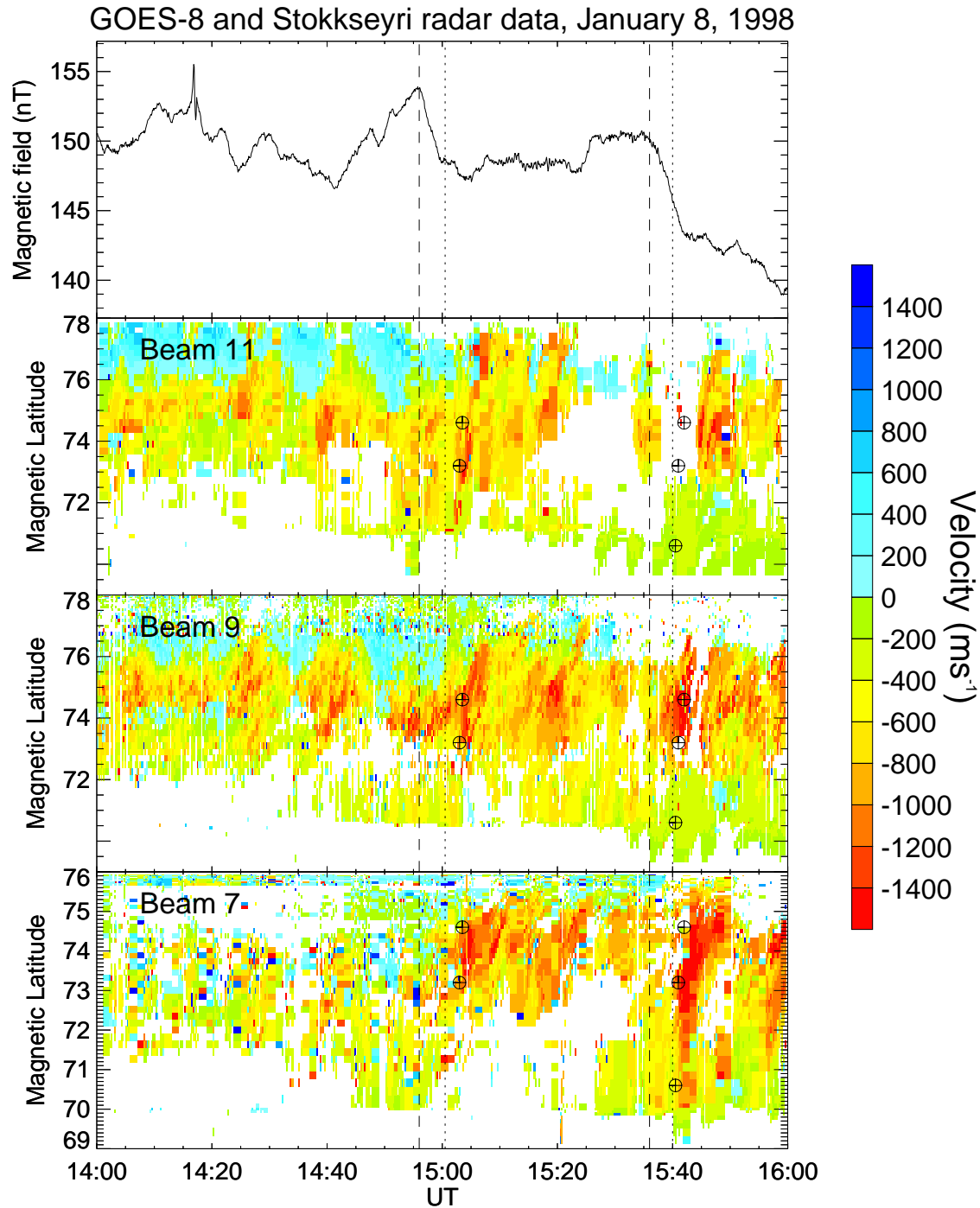


**Plate 1.** A comparison of GOES-8 and SuperDARN data. The first panel shows the total magnetic field measured with GOES-8. Panels two to four show Range-Time plots from Stokkseyri for beams 11, 9 and 7 (see figure 5a). The Stokkseyri Data is shown in magnetic latitude as a function of time. The dashed vertical lines indicate the start of a pressure decrease detected at GOES-8. The dotted vertical lines indicate the start of the main impulse detected by the Greenland magnetometers (approximate timing for the first event). The circled crosses denote the instant of maximum positive deflections of the  $X_M$  component at ATU, STF and GHB, plotted at the magnetometer latitudes.

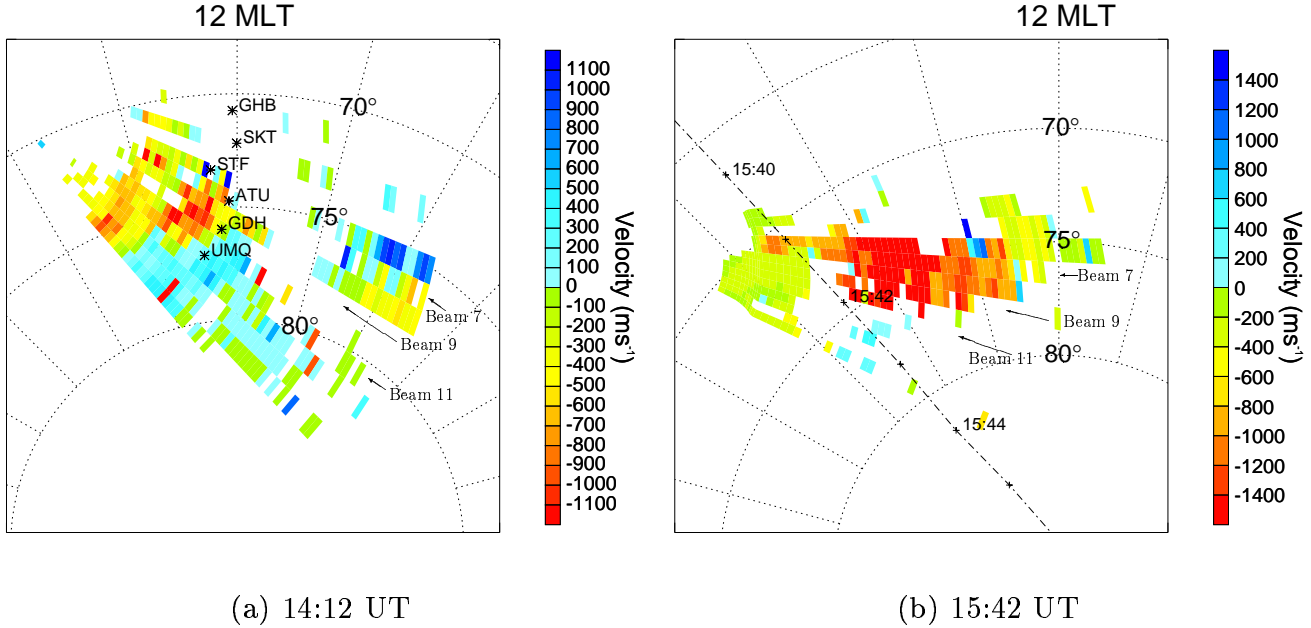


**Figure 5.** The field of view of the Stokkseyri radar, plotted in AACGM magnetic coordinates (see text for explanation) on January 8, 1998. (a) The field of view at 14:12 UT. Several stations from the Greenland magnetometer chain are shown. (b) The dash-dot line shows the path of the NOAA-14 satellite in the field of view at 15:42 UT. Crosses mark the positions at one-minute intervals.

GOES-8 data may also be found to correlate with radar data. The local minima of the magnetic field at 14:25 and 14:42 UT correspond for example to a sunward flow enhancement and a poleward shift of the CRB. The fact that most of the low-latitude magnetometers in figure 3 reproduce the GOES-8 signatures, indicates probably a pressure effect.

The two sunward flow bursts following the pressure decreases observed by GOES-8 at 14:56 and 15:36 UT will now be discussed in more detail. The radar signatures for the latter case will be examined first.

Immediately after 15:40 UT, data from beam 7 show a sharp velocity transition from background velocities to about -1.7 km/s. This indicates a 4 minute lag from the onset of the pressure decrease measured at GOES-8 to the first flow response in the 70° to 76° MLAT range. Incidentally, the main response of the Greenland magnetometers started at 15:40 UT, as indicated by the vertical dotted line in plate 1. The flow response is almost simultaneous from about 70° to 73.5° MLAT. Above 73.5° MLAT, the negative flow response propagates to higher latitudes with time, as suggested by the Greenland magnetometer data. The comparison with the maximum positive magnetic deflections at ATU, STF and GHB (marked by circled crosses in plate 1) shows that the maximum radar response lags the magnetometer data by less than one minute. Although the correspondence in time is not exact, the radar signa-

tures show clearly the same evolution: a response lag that increases with latitude.

The radar data show that the CRB is generally detected between 75.5° and 76.5° MLAT in the 12:00 to 14:00 MLT region. In comparison, the SI/SI<sup>-</sup> current reversal boundary associated with the preliminary and main impulse (deduced from magnetometer data) is near 70° MLAT at 13:52 UT (around 12:00 MLT) and probably below 70° MLAT at 15:42 UT (around 14:00 MLT). This is about 6° lower than the CRB, and indicates that these two boundaries do not coincide.

The velocity signatures of the 15:42 UT burst in beam 9 are lost between 15:43 and 15:46 UT. Data in beam 11 are also lost during most of the event. It is an observational fact [Pinnock et al., 1991, 1995] that SuperDARN echoes are often lost in regions of strongly enhanced convection. Rodger et al. [1994] have suggested that an increased rate of recombination due to effects of high ion flow velocities and the associated Joule heating could be responsible for this by changing either the radar wave propagation or the plasma turbulence responsible for the scatter.

The ionospheric flow response to the 14:56 UT pressure decrease is a bit harder to understand, since it consists of two flow bursts. The first one is rather weak and observation in beam 9 at 15:00 UT show that it is associated with an increase in the CRB latitude. The second flow burst, which starts at 15:03 UT, is stronger

and peaks at about 15:04 UT. This indicates that the delay from the start of the pressure decrease at GOES-8 to the maximum flow response is about 4 and 7 minutes to the weak and strong responses, respectively. The flow response of the 15:04 UT event propagates poleward, as for the 15:42 UT burst. The signatures in beam 9 indicate that the onset is almost simultaneous between  $73^\circ$  and  $74.5^\circ$  MLAT and that there is a 3 minute lag to the onset at  $76^\circ$  MLAT.

The position of the flow bursts with respect to the open/closed field line boundary (OCB) is an important factor when determining whether reconnection is a possible driving mechanism. The analysis of l-o-s Doppler spectral width can be used for this purpose, but only for data originating near the cusp [Baker *et al.*, 1990, 1995]. Unfortunately, this method does not apply to the present data, since it would place the OCB between  $73^\circ$  and  $74^\circ$  MLAT in the 14:00 to 15:20 UT period. This position is up to  $3^\circ$  lower than the CRB and would put all of the high-speed sunward flow on open field lines, which is very unlikely. The spectral width method was developed using radars with mostly meridional beams. It is thus possible that the method either has to be modified for zonal radars like Stokkseyri [Andre *et al.*, 2000], or that the radar is too far from the cusp.

However, the position of the OCB can be evaluated from the l-o-s velocities. The arrival of Alfvén waves from the magnetopause reconnection site causes the flow reversal at the CRB in the ionosphere [e.g. Southwood, 1987; Lockwood, 1997]. If the polar cap boundary in the FOV is adiarcic (i.e. no flow across it), then the positions of the OCB and CRB should be almost identical [e.g. Lockwood, 1997, 1998]. However, if there is flow across the CRB, then time-of-flight and propagation effects have to be considered. Using an Alfvén wave propagation speed of 600 km/s and a  $20 R_e$  distance from the polar cap in the radar FOV to the reconnection point (see Lockwood [1997]), a propagation time of about 210 seconds is obtained. Typical values of the poleward l-o-s velocities in the most meridional radar beam can be used as an estimate of flow speeds across the CRB, and an upper value of 300 m/s is obtained. This indicates that the separation between the OCB and the CRB should not be larger than  $0.6^\circ$  in MLAT. As explained by Lockwood [1998], these two boundaries are expected to move together, so the changes in the position of the CRB detected with the radar probably indicate motions of the OCB as well.

Since the sunward flow bursts originate well equatorward of the CRB, the above analysis indicates that they occur on closed field lines. This will be further examined in the next section.

## NOAA-14 satellite data

The NOAA-14 satellite passed across the FOV of the Stokkseyri radar between 15:40 and 15:44 UT (see figure 5b). At 15:42 UT, the satellite is at about  $74.3^\circ$  MLAT, which is approximately where the highest sunward velocities are detected with the radar.

Figure 6 shows particle measurements from NOAA-14. The first panel shows the total electron energy flux in the 0.3 - 20 keV range. A very sharp rise in the energy flux is observed just before 15:42 UT, and the flux then decreases smoothly in the poleward direction. The middle panel shows the electron differential number flux for 4 different channels in the 300 to 4870 eV range. The data show a high flux of electrons with energies above 773 eV when the energy flux peaks. Of special interest is the high flux of 773-1088 eV electrons at 15:42:01 UT, which is about a factor 3 higher than the flux of 300-458 eV electrons. Since a high flux of electrons with energies above 773 eV are unlikely to be associated with open field lines [e.g. Newell *et al.*, 1991], this indicates that the satellite is on closed field lines at  $74.3^\circ$  MLAT. It is not possible from the electron data to place the OCB exactly, since the variations in the energy and particle flux are rather smooth with time after 15:42 UT. A first guess might however be near the rather sharp decrease in energy flux at 15:42:15 UT.

The ion data can be used to determine the low-altitude signature of the OCB with better precision. The last panel in figure 6 shows the energy of the ions that have the highest particle flux. Due to noise, only data in the 15:41 to 15:43 UT period can be used. From about 15:41 to just after 15:42 UT, the energy is mostly above 10 keV, which indicates that the satellite is on closed field lines. At 15:42:15 UT, the energy suddenly drops and stays mainly below 1 keV until 15:43 UT. This indicates that the passage from trapped ions to magnetosheath ions takes place at around 15:42:15 UT, or at  $75.2^\circ$  MLAT. This occurs at the same time as the observed drop in the electron energy flux, which supports this conclusion. Following Lockwood [1997], this position should also mark the CRB, the OCB being situated at the same latitude (if the polar cap is adiarcic) or slightly below (if diarcic). This position of the CRB is somewhat lower than the CRB inferred from the Stokkseyri data (plate 1). The radar data indicate that the mean position of the CRB is between  $75.5^\circ$  and  $76.0^\circ$  MLAT in the 15:30 to 16:00 UT period. However, as figure 5b shows, the latitude of the CRB changes with the local time (above  $77.5^\circ$  MLAT at 13 MLT and clearly below  $76.0^\circ$  MLAT at 14:30 MLT). This observation is in agreement with the result that changes in the latitude of the CRB propagate tailward. Near the path of the satellite, the positive velocities in the polar cap indicate that the CRB is not poleward of  $75.6^\circ$  MLAT. Considering the errors in the estimations, the two determinations of the CRB agree rather well,

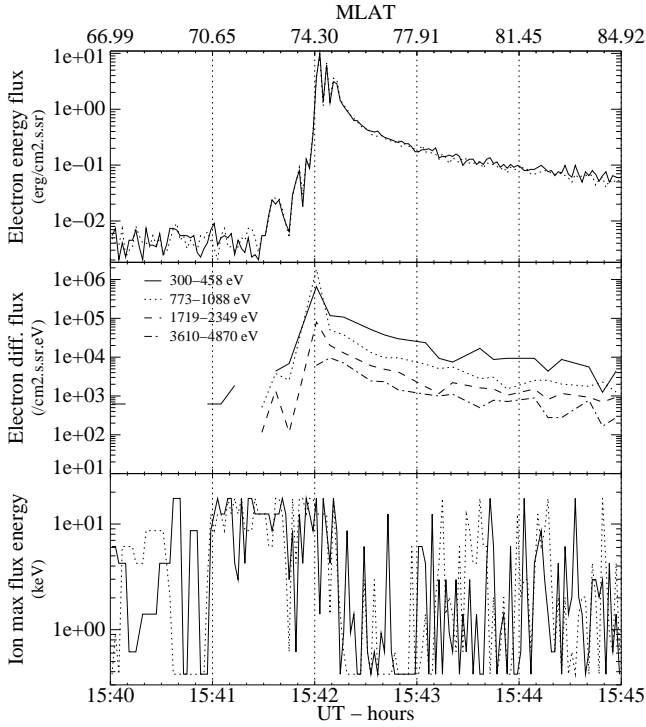


**Figure 6.** NOAA-14 satellite data on January 8, 1998. The upper panel shows electron energy flux in the 0.3 - 20 keV range for pitch angles 0° (solid line) and 30° (dotted line). The middle panel shows differential number flux of 0° pitch angle electrons in four energy bins. The lower panel shows the energy of the ions with the highest particle flux for pitch angles 0° (solid line) and 30° (dotted line).

and it can be placed between 75.2° and 75.6° MLAT at 14:30 MLT and 15:42 UT.

The sunward flow burst at 15:42 UT originates equatorward of this position of the CRB/OCB, and we conclude thus that it occurs on closed field lines. Although no particle data are available at the time of other flow bursts, we conclude from the radar l-o-s velocity analysis that they all occur on closed field lines.

### Summary of observations

In the case studied, the IMF conditions were favorable for low-latitude reconnection and signatures of the expected crescent-shaped flow cell in the afternoon region were observed with the Stokkseyri radar. Global magnetometer responses to solar wind pressure changes were observed. Associated with solar wind pressure decreases, inferred from Wind, GOES-8 and ground magnetometer data, sunward flow bursts in the return flow from the nightside were detected in the 12-15 MLT sector. The flow velocities were up to two to three times larger than the background flow. The sunward flow in-

tensities shift poleward with time, an observation confirmed by Greenland magnetometer data. These flow bursts are simultaneous with the main response (MI) of the Greenland magnetometers. Changes in the position of the convection reversal boundary that drifted tailward were also detected. Poleward shifts of the CRB corresponded to faster sunward flow equatorward of the CRB and equatorward shifts to higher tailward flow poleward of the CRB.

The NOAA-14 satellite data show that the latitude of the OCB is close to the position of the CRB detected by the Stokkseyri radar, and both are located between 75.2° and 75.6° MLAT at 14:30 MLT (15:42 UT). Using the *Araki* [1994] SI/SI<sup>-</sup> model, the Greenland magnetometer chain indicates that the latitude of the current system responsible for the main impulse is lower than 70° MLAT at 15:42 UT, more than 5° equatorward of the OCB. The sunward flow bursts are thus observed on closed field lines, and on the poleward side of the main impulse current system.

## Discussion

### Reconnection as a direct driving mechanism

Although the sunward flow bursts are correlated with pressure decreases, magnetic reconnection cannot be excluded as a driving mechanism beforehand, since pressure changes may stimulate reconnection [Scurry and Russell, 1991]. However, a strong reason for excluding the direct influence of reconnection as a driver is the direction of flow detected in the bursts. The IMF B<sub>y</sub> component is negative during the whole period under study, which means that the magnetic tension should pull reconnected flux tubes towards the evening sector in the northern hemisphere. The corresponding flow channels should thus have a strong eastward component. On the contrary, the flow bursts observed in this study have a clear westward flow direction, which excludes a direct reconnection effect. In addition, the fact that the sunward flow bursts originate on closed field lines (up to 4° equatorward of the OCB) strengthens further the above conclusion.

### Reconnection as an indirect driving mechanism

The ionospheric plasma is considered to incompressible, such that flow excited at the OCB by reconnection can be expected to produce flows poleward and equatorward of that latitude [Southwood, 1987; Cowley and Lockwood, 1992]. Thus, although the flow bursts are located on closed field lines, they could be a consequence of reconnection. Moen *et al.* [1995, 1996] present a case of enhanced sunward flow in the afternoon sector, associated with tailward moving auroral structures at higher latitudes. The authors conclude that the auroral forms were the signatures of reconnection. The tailward speed of the auroral forms was approximately

1.5 km/s, which is of the same order as the tailward phase velocity of the CRB changes determined in the present study. Further, in their study, the sunward flow velocities are west-north-westward, and no discernible flow rotation is associated with the bursts. High flow speeds (2-3 km/s) are detected up to  $2^{\circ}$  equatorward of what is probably the CRB. All these features are similar to the data presented in this study. These authors propose that the enhanced sunward velocities are due to a global response of the ionosphere to pulsed day-side reconnection [Cowley and Lockwood, 1992]. They note that the polar cap boundary motions have a 12-15 minute time period, which is close to the proposed time it should take to reestablish a new equilibrium after transient open flux has been added to the polar cap. In comparison, the mean periodicity of the CRB oscillations on January 8 is about 11 minutes between 14:00 and 14:50 UT.

However, the Stokkseyri radar data shows that the tailward flow poleward of the CRB is weaker and less structured than the sunward flow equatorward of the CRB. It is thus hard to imagine that the tailward flow is the driving mechanism for the sunward bursts. Moen *et al.* [1995, 1996] found also a localized expansion of the polar cap (deduced from optical data) during the events of enhanced sunward convection, whereas our events show the opposite, a localized contraction of the polar cap.

Recently, Milan *et al.* [1999] showed the occurrence of sunward plasma flow patches in the return flow (probably of bursty nature) and related these to sporadic reconnection in the cusp. Although the idea that the return flow away from the cusp can be excited by reconnection agrees with current conceptual models [e.g. Cowley and Lockwood, 1992; Southwood, 1987], these predict a tailward phase propagation of the return flow enhancement, and not sunward as observed by Milan *et al.* [1999]. As in the present case, the flow patches observed by these authors seem to originate from well below the CRB, although it is less clear from their data. Unfortunately, the low temporal resolution of the data and missing solar wind pressure data do not permit an analysis similar to the one carried out in this paper. We may be observing the same phenomenon as Milan *et al.* [1999], but global pressure changes are a more likely trigger in our case, as noted above, and for the reasons given in the next section.

### Pressure changes as a driving mechanism

Moen *et al.* [1995] do not exclude the possibility that the enhanced sunward convection discussed above might be related to pressure changes, and that pressure might also be modulating the reconnection rate. Unfortunately, no solar wind data was available for their study. However, we examined low- and mid-latitude magnetometer data during their event between 12:10

and 12:22 UT period on January 7, 1992, which corresponds to a period when strong sunward flow is detected (cf. figure 5 in their paper). The H-component at different local times shows that there is a global response of the magnetosphere in this period, probably indicating a slight pressure decrease. It is thus possible that pressure decreases are driving the observed sunward flow enhancements. However, a more extended study on other flow enhancements during their day of study will be needed to confirm this hypothesis.

GOES-8 and ground magnetometer data show that the sunward flow bursts are the response to a global magnetosphere phenomena. This points strongly toward solar wind pressure control. Although radar and high-latitude magnetometer data are consistent with the global SI/SI<sup>-</sup> model of pressure influence, a more local approach can also be considered, as discussed in the next section.

**Travelling convection vortices** The motions of the CRB and the sunward flow enhancements might be due to traveling convection vortices (TCVs). Satellite data have shown that TCVs can shift the cusp boundary equatorward by up to  $3^{\circ}$  in latitude [Potemra *et al.*, 1992]. Several authors [e.g. Lühr *et al.*, 1996] have shown that the center of TCV systems maps to closed field lines. Yahnin and Moretto [1996] used satellite data to locate magnetosphere boundaries around TCVs, and showed that the TCV centers map to the central plasma sheet. However, the exact generating mechanism for TCVs is not yet fully elucidated. Lühr *et al.* [1996] propose that a pressure-change generated compressional (expansional) wave at the magnetopause couples to an Alfvén wave at density gradients in the magnetosphere and generates FACs. These authors propose that the FACs form at the inner edge of the low-latitude boundary layer, but the results of Yahnin and Moretto [1996] would rather indicate a FAC generation at the boundary plasma sheet/central plasma sheet boundary.

Both the effect on the CRB and the origin of TCVs on closed field lines, several degrees equatorward of the low-altitude signatures of the OCB, are consistent with the data in this study. The tailward propagation of CRB changes is also in agreement with this picture, although the 2 km/s velocity obtained is slightly lower than typical reported TCV velocities (3-7 km/s). However, the characteristics of the sunward flow bursts do not agree with TCVs being the main driving mechanism for at least two reasons. In a simple double-vortex picture of a TCV, a pressure decrease in the afternoon sector leads to a plasma flow system with a clockwise leading vortex (upward FAC) and an anti-clockwise trailing vortex (downward FAC). The main flow change due to the system should occur between the two FACs, where the flow is mainly poleward. This flow direction does not agree with the sunward flow bursts, which are mainly zonal. This orientation is confirmed

by the Greenland magnetometer data, which indicate that the east-west magnetic deflections (not shown, related to the north-south plasma velocity) are about 2.5 times smaller than those of the north-south component. If the east-west velocities related to TCVs are considerably larger than the north-south velocities (typically  $< 500$  m/s, deduced from magnetometer data), then TCVs could be responsible for the sunward flow bursts. However, observations [e.g. Lühr *et al.*, 1996] do not support this hypothesis, and indicate actually the opposite. Another reason for excluding TCVs as the main source is the fact that the sunward flow bursts do not propagate tailward. A TCV propagating tailward at about 2 km/s should be detected first in beam 7 and then in beam 9 about one minute later. A comparison of the data in these two beams shows that the two large sunward bursts are detected simultaneously, or even slightly earlier in beam 9 than in beam 7. Thus, although TCVs might possibly explain the CRB changes, they are not consistent with the sunward bursts.

**The SI/SI<sup>-</sup> model** The Greenland magnetometers show that in general, the high-latitude afternoon ionosphere reacts to large pressure increases and decreases as predicted by the two-cell SI/SI<sup>-</sup> current model reviewed by Araki [1994], although the full set of signatures of the model is not observed. In particular, the preliminary impulse which is clearly observed at the ground magnetometer NAQ for a positive pressure pulse is not observed for a negative one. Also, the simultaneous variations of the IMF probably masked the magnetic signatures observed following the 14:56 UT pressure decrease. However, the sunward flow bursts in radar data correspond well with the increase in the Greenland X<sub>M</sub>-components, and show a similar behavior with latitude. The highest flow velocities were also detected where the magnetometers showed the strongest response. The flow bursts are associated with the main impulse observed by the magnetometers. The fact that the preliminary impulse is weaker than the main impulse in the ground magnetometer signatures at radar scatter latitudes is consistent with the radar detecting only the main response. It must thus be concluded that the sunward flow bursts fit best with the SI/SI<sup>-</sup> model, and can be explained in terms of ionospheric currents responding to solar wind pressure changes. Other cases similar to the one presented in this paper show also that the pressure control of sunward flow bursts is not an isolated phenomenon.

Figure 7 shows schematically how the main impulse of a pressure decrease influences the electric field in the ionosphere, and thus the convection. The figure shows a view of the northern hemisphere in a plane perpendicular to the earth-sun axis, observed from the sun. The FACs associated with the main impulse are downward at dusk (field line B) and upward at dawn (field line B'). The corresponding electric field ( $\mathbf{E}_{MI}$ ) is directed from

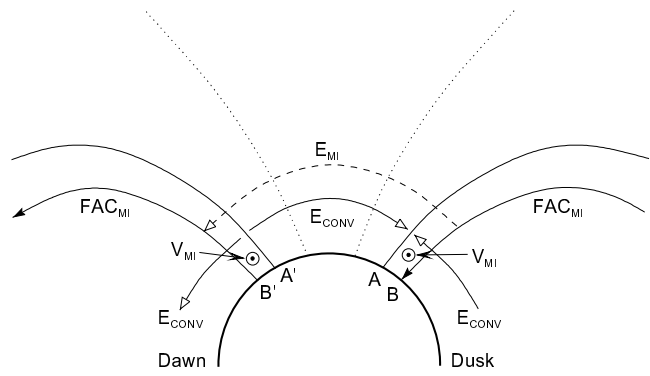


**Figure 7.** Parallel currents and electric fields during the main impulse of a pressure decrease in the magnetosphere. The figure shows the northern hemisphere, as observed from the Sun.

dusk to dawn. Field lines A and A' indicate the position of the CRB before the pressure decrease. The convection electric field ( $\mathbf{E}_{CONV}$ ) is dusk to dawn equatorward of the CRB, and dawn to dusk poleward of the CRB. The schematic illustrates that  $\mathbf{E}_{MI}$  increases the electric field in the latitudinal range between A and B (and between A' and B'), that is between the CRB and the latitude of the main impulse FAC. This increased electric field drives the sunward flow bursts ( $\mathbf{V}_{MI}$ ) in these regions, as observed in the present study. It can also be noted that the main impulse FACs are positioned at region 2 current latitudes [Ujima and Potemra, 1976], have the same flow direction, and should thus reinforce this current.

In conclusion, we have shown that at least some sunward transient convective flows around noon in the ionosphere can be attributed to decreases in solar wind pressure. Although reconnection remains the major source, care has to be taken not to attribute all transient events observed at and near the cusp to reconnection.

**Acknowledgments.** A. Thorolfsson is supported by the EC under the TMR Marie Curie Research Training Grant scheme. M. Pinnock gratefully acknowledges support from the Université Pierre et Marie Curie which facilitated this work. The operation of the Stokkseyri radar is supported by the Institut National des Sciences de l'Univers (INSU). The authors acknowledge K. Ogilvie and R. Leping at NASA for the use of Wind data and R. Zwickl, NOAA/SEL for the use of GOES-8 data. They would also like to thank P. Stauning, DMI for providing Greenland magnetometer data. The NOAA satellite data were originally supplied from NFDC/NOAA and archived by WDC for Aurora in NIPR, Japan. KAK magnetometer data are courtesy of the World Data Center System. Other magnetometer data are courtesy of the INTERMAGNET data service. The authors thank one of the referees for very helpful comments aimed at clarifying the relationship between

the SI/SI<sup>-</sup> model and the data.

## References

Andre, R. A., M. Pinnock, J.-P. Villain, and C. Hanuise, On the factors conditioning the Doppler spectral width determined from SuperDARN HF radars, *Journal of Geomagnetism and Aeronomy*, 2000, in press.

Araki, T., A physical model of the geomagnetic sudden commencement, in *Solar Wind Sources of Magnetospheric Ultra-Low Frequency Waves*, edited by M. J. Engebretson, K. Takahashi, and M. Scholer, vol. 81 of *Geophysical Monograph*, pp. 183–200, American Geophysical Union, Washington DC, USA, 1994.

Araki, T., and H. Nagano, Geomagnetic response to sudden expansions of the magnetosphere, *J. Geophys. Res.*, **93**, 3983–3988, 1988.

Baker, K. B., and S. Wing, A new magnetic coordinate system for conjugate studies at high latitudes, *J. Geophys. Res.*, **94**, 9139–9143, 1989.

Baker, K. B., R. A. Greenwald, J. M. Ruohoniemi, J. R. Dudeney, and M. Pinnock, Simultaneous HF-radar and DMSP observations of the cusp, *Geophys. Res. Lett.*, **17**, 1869–1872, 1990.

Baker, K. B., J. R. Dudeney, R. A. Greenwald, M. Pinnock, P. T. Newell, A. S. Rodger, N. Mattin, and C. I. Meng, HF radar signatures of the cusp and low-latitude boundary layer, *J. Geophys. Res.*, **100**, 7671–7695, 1995.

Berchem, J., and C. T. Russell, Flux transfer events on the magnetopause: Spatial distribution and controlling factors, *J. Geophys. Res.*, **89**, 6689–6703, 1984.

Cowley, S. W. H., and M. Lockwood, Excitation and decay of solar wind-driven flow in the magnetosphere-ionosphere system, *Ann. Geophysicae*, **10**, 103–115, 1992.

Cowley, S. W. H., M. P. Freeman, M. Lockwood, and M. F. Smith, The ionospheric signature of flux transfer events, in *ESA SP-330*, pp. 105–112, ESA, Neuilly, France, 1991.

Erlandson, R. E., D. G. Sibeck, R. E. Lopez, L. J. Zanetti, and T. A. Potemra, Observations of solar wind pressure initiated fast mode waves at geostationary orbit and in the polar cap, *J. Atmos. Terr. Phys.*, **53**, 231–239, 1991.

Glassmeier, K. H., and C. Heppner, Traveling magnetospheric convection twin vortices: Another case study, global characteristics, and a model, *J. Geophys. Res.*, **97**, 3977–3992, 1992.

Glassmeier, K. H., M. Hoenisch, and J. Untiedt, Ground-based and satellite observations of traveling magnetospheric convection twin vortices, *J. Geophys. Res.*, **94**, 2520–2528, 1989.

Goertz, C. K., E. Nielsen, A. Korth, C. Haldoupis, P. Hoeg, D. Hayward, and K. H. Glassmeier, Observations of a possible ground signature of flux transfer events, *J. Geophys. Res.*, **90**, 4069–4078, 1985.

Greenwald, R. A., et al., DARN/SuperDARN: A global view of the dynamics of high-latitude convection, *Space Sci. Rev.*, **71**, 761–796, 1995.

Iijima, T., and T. A. Potemra, Field-aligned currents in the dayside cusp observed by Triad, *J. Geophys. Res.*, **81**, 5971–5979, 1976.

Karlson, K. A., M. Øieroset, J. Moen, and P. E. Sandholt, A statistical study of flux transfer event signatures in the dayside aurora: The IMF B<sub>y</sub>-related prenoon-postnoon asymmetry, *J. Geophys. Res.*, **101**, 59–68, 1996.

Kikuchi, T., Evidence of transmission of polar electric fields to the low latitude at times of geomagnetic sudden commencements, *J. Geophys. Res.*, **91**, 3101–3105, 1986.

Kikuchi, T., T. Araki, H. Maeda, and K. Maekawa, Transmission of polar electric fields to the equator, *Nature*, **273**, 650, 1978.

Kivelson, M. G., and D. J. Southwood, Ionospheric traveling vortex generation by solar wind buffeting of the magnetosphere, *J. Geophys. Res.*, **96**, 1661–1667, 1991.

Korotova, G. I., D. G. Sibeck, T. Moretto, and G. D. Reeves, Tracking transient events through geosynchronous orbit, *J. Geophys. Res.*, **104**, 10,265–10,273, 1999.

Lockwood, M., Identifying the open-closed field line boundary, *J. Geophys. Res.*, **102**, 17,475–17,487, 1997.

Lockwood, M., Identifying the open-closed field line boundary, in *Polar Cap Boundary Phenomena*, edited by J. Moen, A. Egeland, and M. Lockwood, vol. 509 of *NATO ASI series*, pp. 73–90, Kluwer Academic Publishers, Dordrecht, The Netherlands, 1998.

Lockwood, M., P. E. Sandholt, S. W. H. Cowley, and T. Oguti, Interplanetary magnetic field control of dayside auroral activity and the transfer of momentum across the dayside magnetopause, *Planet. Space Sci.*, **37**, 1347–1365, 1989.

Lockwood, M., S. W. H. Cowley, P. E. Sandholt, and R. P. Lepping, The ionospheric signatures of flux transfer events and solar wind dynamic pressure changes, *J. Geophys. Res.*, **95**, 17,113–17,135, 1990.

Lühr, H., M. Lockwood, P. E. Sandholt, T. L. Hansen, and T. Moretto, Multi-instrument ground-based observations of a travelling convection vortices event, *Ann. Geophysicae*, **14**, 162–181, 1996.

Milan, S. E., M. Lester, R. A. Greenwald, and G. Sofko, The ionospheric signature of transient dayside reconnection and the associated pulsed convection return flow, *Ann. Geophysicae*, **17**, 1166–1171, 1999.

Moen, J., D. P. E. Sandholt, M. Lockwood, W. F. Denig, U. P. Lovhaug, B. Lybekk, A. Egeland, D. Opsvik, and E. Friis-Christensen, Events of enhanced convection and related dayside auroral activity, *J. Geophys. Res.*, **100**, 23,917–23,934, 1995.

Moen, J., M. Lockwood, P. E. Sandholt, U. P. Lövhaug, W. F. Denig, A. P. Van Eyken, and A. Egeland, Variability of dayside high latitude convection associated with a sequence of auroral transients, *J. Atmos. Terr. Phys.*, **58**, 85–96, 1996.

Newell, P. T., E. R. Sanchez, C. I. Meng, W. J. Burke, M. E. Greenspan, and C. R. Clauer, The low-latitude boundary layer and the boundary plasma sheet at low altitude: Prenoon precipitation regions and convection reversal boundaries, *J. Geophys. Res.*, **96**, 21,013–21,023, 1991.

Øieroset, M., H. Lühr, J. Moen, T. Moretto, and P. E. Sandholt, Dynamical auroral morphology in relation to ionospheric plasma convection and geomagnetic activity: Signatures of magnetopause x line dynamics and flux transfer events, *J. Geophys. Res.*, **101**, 13,275–13,292, 1996.

Øieroset, M., P. E. Sandholt, H. Lühr, W. F. Denig, and T. Moretto, Auroral and geomagnetic events at cusp/mantle latitudes in the prenoon sector during positive IMF B<sub>y</sub> conditions: Signatures of pulsed magnetopause reconnection, *J. Geophys. Res.*, **102**, 7191–7205, 1997.

Pinnock, M., A. S. Rodger, J. R. Dudeney, R. A. Greenwald, and K. B. Baker, An ionospheric signature of possible enhanced magnetic field merging on the dayside magnetopause, *J. Atmos. Terr. Phys.*, **53**, 201–212, 1991.

Pinnock, M., A. S. Rodger, J. R. Dudeney, K. B. Baker, P. T. Newell, R. A. Greenwald, and M. E. Greenspan, Observations of an enhanced convection channel in the cusp ionosphere, *J. Geophys. Res.*, **98**, 3767–3776, 1993.

Pinnock, M., A. S. Rodger, J. R. Dudeney, F. Rich, and K. B. Baker, High spatial and temporal resolution observations of the ionospheric cusp, *Ann. Geophysicae*, **13**, 919–925, 1995.

Potemra, T. A., R. E. Erlandson, L. J. Zanetti, R. L. Arnoldy, J. Woch, and E. Friis-Christensen, The dynamic cusp, *J. Geophys. Res.*, **97**, 2835–2844, 1992.

Rijnbeek, R. P., S. W. H. Cowley, D. J. Southwood, and C. T. Russell, A survey of dayside flux transfer events observed by ISEE 1 and 2 magnetometers, *J. Geophys. Res.*, **89**, 786–800, 1984.

Rodger, A. S., M. Pinnock, J. R. Dudeney, and K. B. Baker, A new mechanism for polar patch formation, *J. Geophys. Res.*, **99**, 6425–6436, 1994.

Russell, C. T., and R. C. Elphic, Initial ISEE magnetometer results: Magnetopause observations, *Space Sci. Rev.*, **22**, 681–715, 1978.

Russell, C. T., and R. C. Elphic, ISEE observations of flux transfer events at the dayside magnetopause, *Geophys. Res. Lett.*, **6**, 33–36, 1979.

Sandholt, P. E., C. S. Deehr, A. Egeland, B. Lybekk, and R. Viereck, Signatures in the dayside aurora of plasma transfer from the magnetosheath, *J. Geophys. Res.*, **91**, 10,063–10,079, 1986.

Sandholt, P. E., J. Moen, A. Rudland, D. Opsvik, W. F. Denig, and T. Hansen, Auroral event sequences at the dayside polar cap boundary for positive and negative interplanetary magnetic field  $B_y$ , *J. Geophys. Res.*, **98**, 7737–7755, 1993.

Scurry, L., and C. T. Russell, Proxy studies of energy transfer to the magnetosphere, *J. Geophys. Res.*, **96**, 9541–9548, 1991.

Sibeck, D. G., A model for the transient magnetospheric response to sudden solar wind dynamic pressure variations, *J. Geophys. Res.*, **95**, 3755–3771, 1990.

Sibeck, D. G., and J. Croley, D. J., Solar wind dynamic pressure variations and possible ground signatures of flux transfer events, *J. Geophys. Res.*, **96**, 1669–1683, 1991.

Southwood, D. J., The ionospheric signature of flux transfer events, *J. Geophys. Res.*, **92**, 3207–3213, 1987.

Wilken, B., C. K. Goertz, D. N. Baker, P. R. Higbie, and T. A. Fritz, The SSC on July 29, 1977 and its propagation within the magnetosphere, *J. Geophys. Res.*, **87**, 5901–5910, 1982.

Yahnin, A., and T. Moretto, Travelling convection vortices in the ionosphere map to the central plasma sheet, *Ann. Geophysicae*, **14**, 1025–1031, 1996.

---

This preprint was prepared with AGU's LATEX macros v5.01, with the extension package 'AGU++' by P. W. Daly, version 1.6b from 1999/08/19.

A. Thorolfsson and J.-C. Cerisier, CETP, 4 avenue de Neptune, 94107 Saint-Maur CEDEX, France

M. Pinnock, BAS, High Cross, Madingley Rd., Cambridge CB3 OET, United Kingdom

Received November 22, 1999; revised March 15, 2000; accepted May 9, 1999.